On Secondary Structure Rearrangements and Equilibria of Small RNAs

Ronald Micura* and Claudia Höbartner[a]

Introduction

RNA structures often implicate a complex folding pathway to reach the minimum free energy state. An understanding of the process of folding is of major significance as this process may reveal dynamic features of an RNA that are directly correlated to functional properties.

An hierarchical model for the folding of RNA has been established that is derived from early studies on tRNA and is consistent in the first order with more recent studies on ribozymes.[1] This model claims that two major structural changes occur on the way from an unfolded RNA molecule to the native state. Stable secondary structures, such as hairpins, are formed rapidly on a microsecond timescale. Tertiary folding then takes place by assembly of the secondary structural elements through long-range base-pairing interactions. This procedure is slower; the acquisition of tertiary interactions occurs on a timescale on the order of milliseconds to seconds.

During the last few years, great efforts have been made to explore RNA folding mechanisms by applying advanced techniques such as single-molecule fluorescence,[2] synchrotron hydroxyl radical footprinting,[3] or temperature gradient gel electrophoresis.[4] The hierarchical model of RNA folding has to be refined in several aspects. Particularly for larger RNAs, the folding can be retarded significantly by the formation of kinetically favorable metastable intermediate structures. The refolding of a trapped intermediate usually involves breakage of base pairs and is therefore energetically costly. In this context, the 'kinetic partitioning mechanism' proposes that different initial starting structures of the unfolded RNA chain are populated, which leads to different but parallel folding pathways and therefore to a mixture of correct and incorrect conformations.[5, 6] The refolding of the incorrect structures may take up to minutes or longer. Moreover, it has to be considered that RNA folding in vivo depends on transcription elongation and is therefore a sequential process.[7] As the rate of transcription (5 – 50 nucleotides (nt) per second for eucaryotic polymerases;[8] 250 nt s^{-1} for bacterial polymerases)[9] is relatively slow compared to the rate of hairpin formation, the partially synthesized chain can favor formation of structures that turn metastable as soon as the chain is complete.

Not least, the influence of the environment accounts for RNA folding. Although it is well known that Mg^{2+} ions have a major impact on the formation of tertiary interactions,[10] it has also been demonstrated that Mg^{2+} ions are responsible for a secondary structure rearrangement in the P5abc subdomain of the *Tetrahymena thermophila* Group I intron ribozyme.[11]

The potential of RNA sequences to fold into metastable structures beside the minimum free energy structure has been exploited by nature in a functional manner. There is evidence that several biologically important RNAs have evolved to use a switch in their secondary structure for regulation of gene function.[12, 20–25]

Self-Induced RNA Switches

A self-induced RNA structural switch is defined as starting from a metastable structure that allows or blocks a particular function of RNA (see **1**, Scheme 1).[12] Thereafter, a structural element becomes available that induces a transition into a stable conformation, which is accompanied by a loss or gain of function (see **2**, Scheme 1). The structural element can be a sequence partition that becomes available during the sequential process of transcription through strand displacement or branch migration (compare **1** and **2**, Scheme 1).

The most intensively investigated secondary (and tertiary) structure rearrangements in RNA concern the folding pathway of the *Tetrahymena* Group I intron[13–16] and the hepatitis delta virus ribozyme,[17–19] regulation of translation of the genomic RNA in bacteriophage MS2,[20, 21] transcriptional regulation of the tRNA synthetase gene in *Bacillus subtilis*,[22, 23] and replication of the HIV genomic RNA.[24, 25]

Another illustrative example is the control of R1 plasmid maintainance in *Escherichia coli* (Scheme 1).[26–28] If the R1 plasmid gets lost in the cell the so-called host-killing (Hok) toxin is expressed and cell death is induced.[29] Expression of the *hok* toxin gene must therefore be controlled at all stages of the lifecycle of the corresponding *hok* mRNA to avoid premature killing of plasmid-containing cells. In part, this control is achieved by an antisense antidote RNA, the suppression-of-killing (*sok*) RNA **4**. The *sok* RNA is transcribed from the R1 plasmid and can bind to the *hok* RNA in the active conformation, which leads to degradation of the resulting duplex by RNase III.[30]

In plasmid-containing cells the fully transcribed *hok* mRNA adopts a stable, highly structured fold **2** that is inactive for translation of the Hok toxin (Scheme 1).[31] This structure is stabilized because of base pairing of an untranslated sequence

[a] *Prof. Dr. R. Micura, Dipl. Ing. C. Höbartner*
University of Innsbruck
Institute of Organic Chemistry
Innrain 52a, Innsbruck (Austria)
Fax: (+43) 512-5072892
E-mail: ronald.micura@uibk.ac.at

  DOI: 10.1002/cbic.200300664

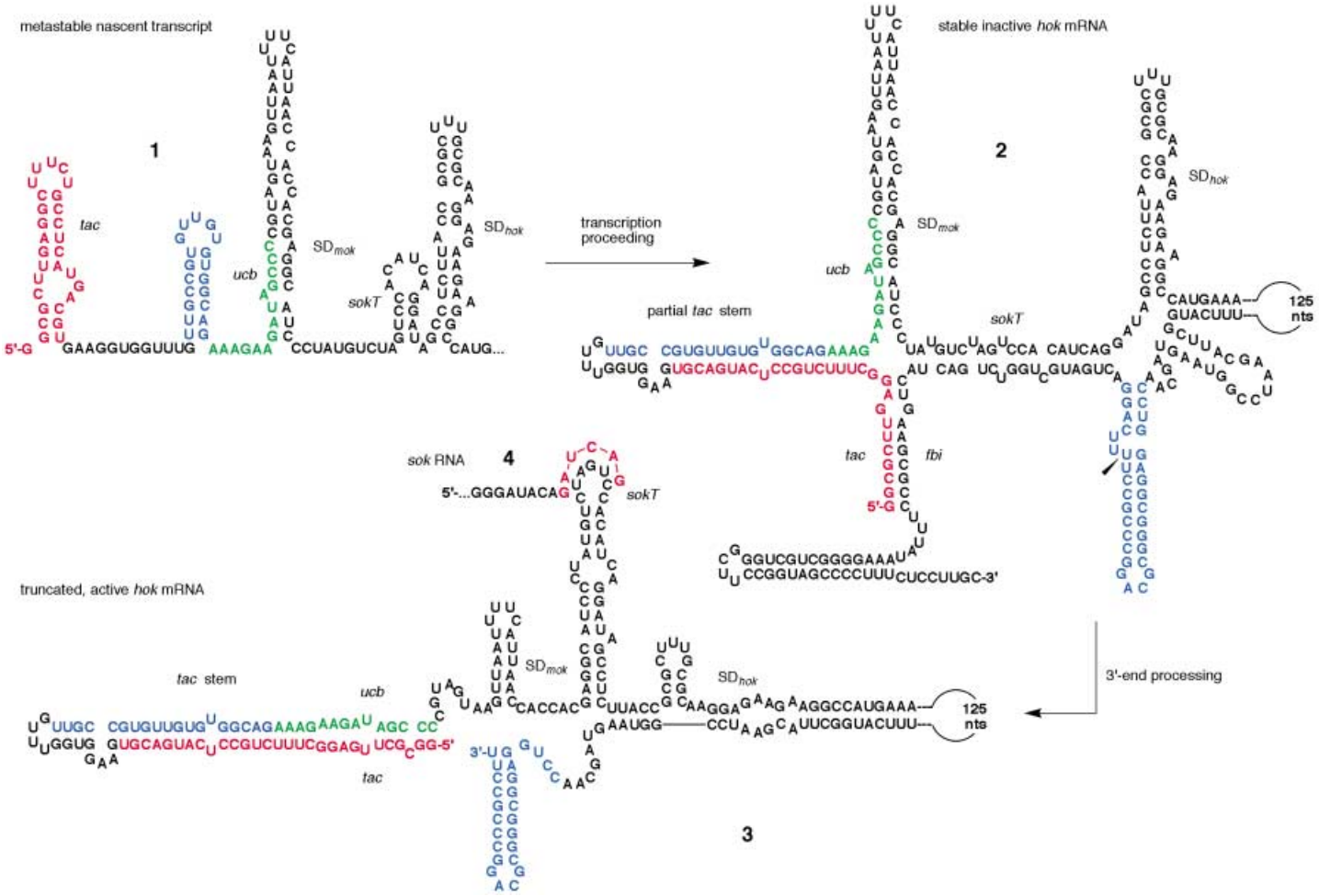

Scheme 1. *The folding pathway proposed for the host killing (*hok*) mRNA: During transcription the* hok *mRNA first forms metastable hairpins at the 5′-end,* ***1****. Once the* hok *mRNA is transcribed to its full length, a secondary structure rearrangement into the stable conformation* ***2*** *takes place by pairing of the 3′-end to the 5′-end. Processing of the 3′-end sequence induces a further secondary structure rearrangement into* ***3****, which finally provides the complete translation activation (*tac*) stem and therefore access to ribosomes.*[12] *Further details are given in the text.* ucb, *upstream complementary box;* sokT, *supression of killing target site;* mok, *modulation of killing; SD, Shine – Dalgarno box;* fbi, *folding back inhibitory element.*

partition at the 3′-end, the folding back inhibitory (*fbi*) element, to the untranslated 5′-end.[32] Thereby, a cloverleaf structure is formed that is highly resistant to degradation. However, after some time, the 3′-end gets processed and degraded, which causes a decisive secondary structure rearrangement.[33] As a result, the active conformation **3** is achieved by formation of a stable translation activator (*tac*) stem and by making the Shine – Dalgarno (SD$_{hok}$) sequence more easily available. This structure is then accessible to ribosomes but also to the antidote *sok* RNA **4** (Scheme 1). In plasmid-containing cells where *sok* RNA is transcribed from the plasmid, the corresponding *hok*/*sok* RNA interaction is responsible for suppressing expression of the Hok toxin. In contrast, in plasmid-free cells, *sok* RNA is not transcribed anymore, gets depleted, and no longer suppresses the translation of the activated *hok* mRNA. This process finally leads to cell death.

What has not been discussed so far is how the *hok* mRNA achieves the *inactive stable* fold **2** with the *fbi* sequence section at the 3′-end pairing to the 5′-end (Scheme 1). The nascent *hok* mRNA transcript is trapped in the metastable conformation **1** as long as the *fbi* sequence partition is not available.[26] Once the *fbi* sequence partition is transcribed, refolding into the inactive stable fold **2** takes place. Importantly, the metastable fold **1** already prevents the formation of the complete translation activator (*tac*) stem through base pairing of the 3′-end nucleotides (upstream complementary box; *ucb*) of the activator stem sequence with a more downstream sequence that comprises the SD box (Scheme 1).[12] In this manner, no access of ribosomes to the growing mRNA chain is possible and the *sok* target region is also inaccessible.

The regulation mechanism of the *hok*/*sok* system therefore includes two mRNA structural switches; one originates from the growing transcript because of sequential folding (**1** into **2**), the other is induced in *trans*, which involves 3′-end processing (**2** into **3**). This complex process is necessary to permit the formation of a pool of *hok* mRNAs large enough to destroy plasmid-free cells.[12]

The *hok*/*sok* RNA switch of the growing transcript (**1** into **2**) has also been investigated with respect to kinetics.[26] The switching sequence involves a stretch of only about 70

nucleotides. Temperature jump experiments were used to trap the metastable fold of this individual sequence and the kinetics of refolding into the stable fold were roughly estimated. Importantly, the individual secondary structures involved were proposed on the basis of enzymatic structural footprinting methods.[26] More recently, a pH-jump method was developed for further investigation of the *hok*/*sok* RNA refolding kinetics.[34] A denaturated fold is claimed to be obtained at a low pH value that turns into the metastable fold after a jump to neutral pH. The UV absorbance decay was then used to measure refolding into the stable conformation. In our opinion, the pH-jump method is a valuable step in the search for methods that allow extraction of kinetic data for RNA secondary structure rearrangements occuring on a timescale of minutes to hours. However, this example also demonstrates the lack of methodologies that focus on direct structural parameters to measure such RNA refolding kinetics. Suitable approaches would demand RNA secondary structure probing by NMR spectroscopy. Before we discuss such an approach we address an artificially created RNA sequence that satisfies two different secondary structure models, each of which has a distinct function. The two different reactivities observed for this RNA sequence suggest that two different folds are significantly populated at the same time.

One Sequence, Two Ribozymes

Bartel and co-workers have presented an RNA sequence that can adopt either of two ribozyme folds and can catalyze two different reactions (Scheme 2).[35] One reaction is the cleavage of RNA catalyzed by the hepatitis delta virus (HDV) ribozyme, which assists the replication of HDV viral RNA. The other reaction is RNA ligation catalyzed by the class III ligase ribozyme, an activity obtained in the laboratory by in vitro selection experiments. The two ribozyme folds are completely different and do not share a single base pair. Importantly, minor variants of this sequence are highly active for one or the other catalytic activity and can be accessed from the prototype by only a few nucleotide mutations.[35]

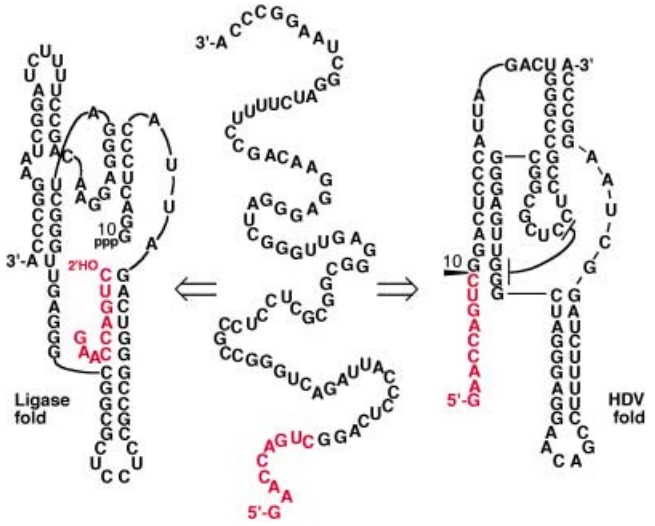

Scheme 2. *The artificially created RNA sequence satisfies two different secondary structures, each associated with a different ribozyme activity. Cleavage of the 88-nt RNA catalyzed by the hepatitis delta virus (HDV) fold, and ligation of the 9-nt substrate to the 79-nt strand by the class III ligase fold have been assayed individually, and results suggest that the two folds are coexisting.*[35]

Experimentally, the two folds of the 88-nt sequence have been read out through the different ribozyme activities. For the ligase fold, the ligation reaction of the corresponding 79-nt RNA with a 5′-triphosphate moiety and the ^{32}P-labeled 9-nt substrate was followed by denaturating gel electrophoresis and quantified with a phosphorimager. The cleavage reaction of the full-length ^{32}P-labeled RNA was analyzed under the same reaction conditions.[35]

Biological activities cannot provide quantitative information on the populations of the individual folds. A low activity can either be explained by a small fraction of molecules populating a ribozyme fold or by a suboptimal active site within molecules that do not fold properly. Structural probing with a Pb(II) cleavage assay indicated that both explanations are relevant.[35] Moreover, it remains a challenging question whether a structural rearrangment into the HDV fold that catalyzes the cleavage reaction takes place upon ligation and vice versa. The folding problem for this artificial ribozyme sequence makes clear again that direct structural data for alternative RNA folds and quantitative data concerning the populations involved are usually not available and that the development of methods to approach this task is desirable.

Secondary Structure Ambivalence of Small RNAs

It has recently been demonstrated that even very small RNAs containing only 18 – 21 nucleotides have the potential for structural ambivalence.[36, 37] A purely rational sequence design was envisaged, with the challenge to find the minimum size of an RNA that is still able to appear in different defined shapes. The design was based on two common secondary structure motifs, namely a GNRA and an UNCG hairpin set in competition with each other (Scheme 3 a). For this purpose, the 3′-end nucleotide sequence of one hairpin was chosen to be identical to the 5′-end nucleotide sequence of the competing hairpin (Scheme 3 a, red part of the sequence). As a further prerequisite, both hairpin motifs were selected to possess comparable base pairing

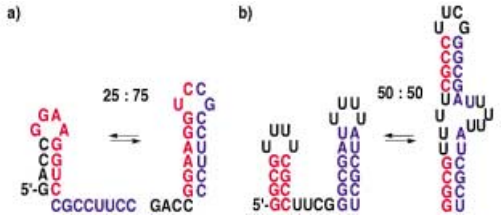

Scheme 3. *Rationally designed small bistable RNAs. a) The 5′ sequence GACC (black) and the 3′ sequence CGCCUUCC (blue) of the 20-nt RNA compete for base pairing with the center sequence GGAAGGUC (red); b) The 32-nt RNA involves the majority of the pairing nucleotides in one conformation in base pairing within the other conformation (red and/or blue base pair combinations) as well.*[37, 38] *The individual populations have been quantified experimentally; see Figure 1.*

stabilities. The stabilities were experimentally verified by determination of thermodynamic parameters for the corresponding truncated reference hairpins by UV melting curve analysis.[36, 37] This technique, however, was unsuccessful in verification of the bistable nature of the complete sequence, as were gel shift assays under native conditions. Therefore, a combined (synthetic and spectroscopic) approach based on a set of reference sequences and comparative ^{1}H NMR spectroscopy was developed and turned out to be most efficient.[38]

Structural Probing by Comparative Imino Proton NMR Spectroscopy

RNA secondary and tertiary structure probing is usually based on enzymatic and chemical footprinting methods.[39, 40] These methods need only small sample amounts for analysis and provide a powerful tool for structural probing, especially of large RNAs for which NMR and crystallographic analyses become difficult. The limitations of footprinting methods mostly concern the specificities of the enzymes and the reactivities of the probes, which are not always well understood.

The conformers of short bistable RNAs are expected to exist in a dynamic equilibrium with a low energy barrier for their interconversion, although this process involves breakage and formation of different base pairs. The timescale for the exchange of conformers is not slow enough to be verified by gel shift assays or UV melting experiments. Chemical and enzymatic structural footprinting methods are also not suitable in this context. However, the timescale of interconversion of secondary structures of small RNAs is expected to be on the order of milliseconds to seconds and minutes, which allows analysis of such conformational equilibria by means of ^{1}H NMR spectroscopy. At this point, we stress the fact that only equilibria of slowly interconverting RNA conformers (> 10 ms) are recognized by the approach described below as this technique relies on the slow exchange regime of NMR. Faster interconverting species provide average signals and these equilibria will therefore not be recognized (fast exchange regime).

The N*H*···N (imino) proton resonances of an RNA appear between 10 and 15 ppm, directly reflect the Watson – Crick base-paired double helical regions and are, in principle, sufficient to verify a secondary structure model (Figure 1 b).[11, 18, 41–44] The assignment of the resonances is a prerequisite and usually requires ^{15}N-labeled RNA samples and advanced NMR methods.[18] A different approach with a pronounced chemical viewpoint has been presented by our group (Figure 1 a).[38] The

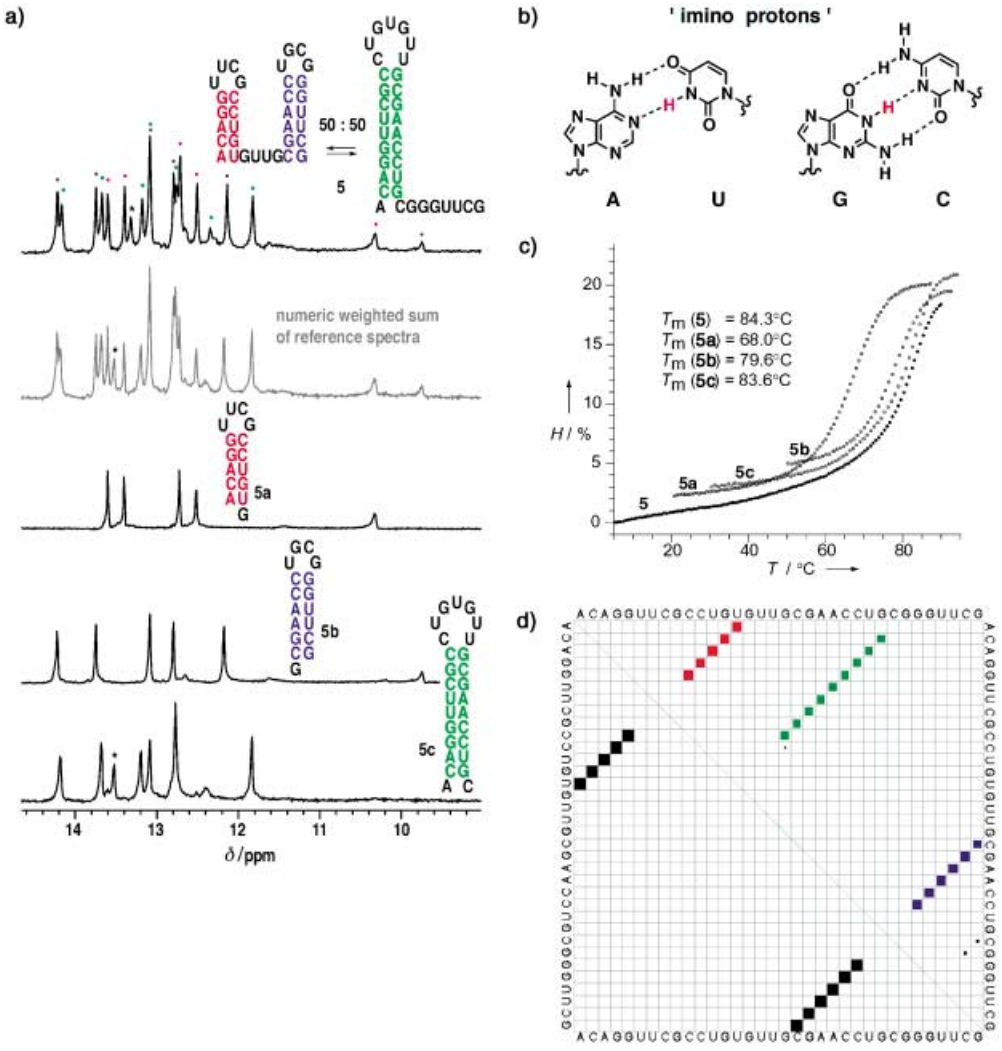

Figure 1. *The 34-nt RNA **5** exists in a monomolecular conformational equilibrium as has been demonstrated by structural probing on the basis of comparative imino proton NMR spectroscopy;[38] a) The individual reference oligoribonucleotides (**5a**, **5b**, and **5c**) are able to adopt only one defined secondary structure and give stemwise sets of imino proton resonances. The numeric, weighted sum of the reference spectra (trace in gray) permits direct comparision with the spectrum of the complete RNA and allows quantification of the equilibrium position with a high degree of accuracy (298 K, in 25 mM sodium arsenate buffer, pH 7.4, H_2O/D_2O, 9:1); b) The so-called 'imino protons' of Watson – Crick base pairs (red); c) The melting profile of **5** does not give evidence for the bistable nature of this sequence. Interestingly, the melting temperatures of the individual double-helical segments are all lower than that of **5**. T, temperature; H, hyperchromicity (250 nm); d) Dotplot for sequence **5** generated by the RNAfold program (Vienna RNA package).[55] The lower left triangle shows the base pairs of the minimum free energy structure. The upper right triangle represents the frequencies of each base pair within the ensemble of all possible structures. Thus, the area of the squares is proportional to pairing probability.*

high thermodynamic stability of the secondary structure compared to that of the tertiary structure of an RNA allows segmentation into the individual Watson–Crick base-paired double helices. The separately synthesized reference oligonucleotides are easily defined as hairpins for terminal stem-loop segments. For internal double-helical tracks of a larger RNA, reference oligonucleotides can also be defined by double-helical sequence homologues with nonnucleotide linker units such as hexa- or heptaethylene glycol phosphates.[45, 46] The spectra of the individual references provide a characteristic fingerprint of imino resonances and enable a stemwise assignment of resonances within the complex NH spectrum of the complete RNA. This approach ('structural probing by comparative imino proton NMR spectroscopy') is very reliable for the assignment and quantification of the equilibrium position of small bistable RNAs and is highly promising for extension to the verification of secondary structure models of larger RNAs. The limitations of this approach will be encountered in cases with complex tertiary structures involving nucleobase triplets or long-distance nucleobase interactions for which simple reference sequences are not easily accessible. In addition, signal overlap will most likely restrict RNA sequence length to less than about 80 nucleotides for the comparative approach. Preliminary experiments suggest that this size is feasible for native RNA secondary structure switches but limitations are encountered for RNAs with a more complex tertiary structure.

UV Melting Profiles and Conformational Analysis

Detailed studies on small bistable RNAs demonstrated that UV melting profile analysis does not allow reliable deduction of their secondary structures. We stress this fact because quite frequently interpretations on the conformational behavior of RNAs are based on melting curves alone. For example, sequence **5** equally populates two different secondary structures at room temperature, as was unequivocally ascertained by comparative imino proton NMR spectroscopy. This sequence displayed a single sigmoid melting profile (and a corresponding first derivative profile with a single inflection point) despite the fact that the melting temperatures of the individual double-helical references **5a**, **5b**, and **5c** differed by more than 15 °C (Figure 1c).

The secondary structure model for the 32-nt sequence depicted in Scheme 3b is comprised of four individual double-helical segments distributed over two equally populated conformers at room temperature. Only the weakest double-helical segment ($T_{m1} = 56$ °C) was separately reflected in a melting profile of biphasic shape.[38] The melting transitions of the remaining three double-helical segments differed by 20 °C ($T_{m2,3,4} = 69$ °C, 75 °C, 89 °C) but were not resolved in the melting profile of the complete sequence. Not even the hyperchromicities of the individual segments were reflected in an additive manner, so that even the biphasic shape with two melting transitions ($T_m = 55$ °C, 85 °C) of comparable hyperchromicities was misleading and favored the expanded conformation.[38]

Secondary Structure Predictions

Computational methods have been developed by several research groups to explore the conformational energy landscapes and the statistical thermodynamics of RNA secondary structure folding.[47–54] Structural probing of small RNAs by comparative imino proton NMR spectroscopy allows direct comparison of the experimental results with predictions obtained by algorithms that cope with the existence of multiple secondary structures. We applied a suboptimal folding algorithm of the Vienna RNA package[55] to generate a list of all suboptimal secondary structures of a given sequence within a desired energy range above the minimum free energy.[56, 57] The partition function algorithm of the RNAfold program then yielded the base pairing probabilities in a Boltzmann-weighted ensemble of all possible structures. As an example, the graphical output, denoted 'dotplot', is shown in Figure 1d for sequence **5**. The dotplot represents the base pair probability matrix. The lower-left triangle shows only base pairs contained in the minimum free energy structure. The upper right triangle represents the frequencies of each base pair within thermodynamic equilibrium. Thus, the area of the squares is proportional to pairing probability. The algorithms recognize the bistable nature of small RNA sequences fairly well. The predicted positions of the equilibria, however, often deviate from the experimentally observed populations of the competing secondary structures.[37, 38]

Impact of Nucleoside Modifications on the Secondary Structure of RNA

The influence of naturally occurring nucleoside modifications on RNA structure is generally believed to be a minor one. The high tolerance and adaptability of RNA with respect to nucleobase mismatches may suggest that modified nucleosides only provide the potential for local conformational modulations of an existing RNA fold. However, there are a few examples that clearly indicate a high impact of nucleoside modifications on the secondary structure of certain biologically relevant RNAs.

The human mitochondrial $tRNA^{Lys}$ possesses six modified nucleosides, namely 1-methyl adenosine at position 9, N^2-methyl guanosine at position 10, two pseudouridine residues at positions 27 and 28, a hypermodified adenosine residue in position 37, and a not-further-characterized modified uridine residue at position U34 (Scheme 4). This tRNA folds into the expected cloverleaf. The corresponding in vitro transcript does not fold into a cloverleaf structure but into an extended bulged hairpin.[58] This noncanonical fold was established by chemical and enzymatic structure probing and consists of an extended amino acid acceptor stem, an extra large loop instead of the T-stem and loop, and an anticodon-like domain. Hence, the modified nucleosides are required for, and responsible for the cloverleaf structure. Moreover, the corresponding tRNA sequence was synthesized with a sole modification, namely a 1-methyl adenosine residue in position 9, by an enzymatic ligation approach. Chemical and enzymatic structure probing demonstrated that this chimeric RNA folded correctly.[59] The

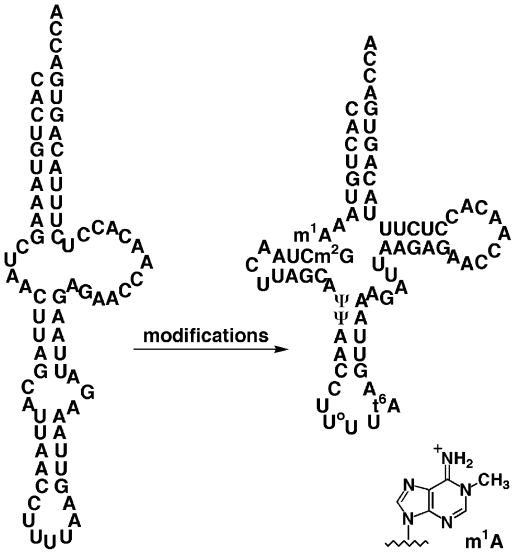

Scheme 4. *The naturally occurring modified nucleoside 1-methyladenosine is responsible for the biologically active cloverleaf fold of a mitochondrial tRNA.[58, 59] Experimental verification of the folds was based on structural probing by chemical and enzymatic footprinting methods. m^1A, 1-methyladenosine; m^2G, N^2-methyl guanosine, Ψ, pseudouridine, t^6A, N^6-threonylcarbamoyl-adenosine, U°, modified uridine not structurally characterized.*

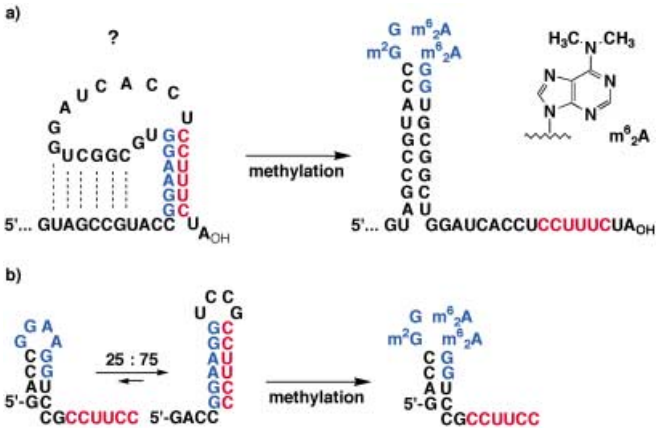

Scheme 5. *a) The Helix 45 motif is located at the 3′-end of the small subunit ribosomal RNA. The successively dimethylated adenosine residues within the tetraloop are conserved in most organisms (e.g.* B. stearothermophilus*). The reason for the methylation is unclear. One hypothesis is that misfolded or partially misfolded structures might be avoided because of the presence of the methylated nucleosides; b) Upon methylation, according to the naturally occuring pattern,*

single methyl group is responsible for disrupting a Watson–Crick A/U base pair in the acceptor stem of the T7 transcript and is therefore sufficient to induce the cloverleaf folding of this tRNA sequence.

It is also likely that the methylation pattern of Helix 45 in the small ribosomal subunit may assist in correct folding, as was suggested based on results for short model sequences.[37] In most organisms the original GGAA loop of Helix 45 is modified by replacement of the adenosine residues with N^6,N^6-dimethyladenosine units. This methylation affects the Watson–Crick pairing face and may prevent unfavorable pairing interactions of the loop with the single-stranded terminal 3′-end sequence (Scheme 5).

In another study, single nucleotides of the inner core of a short palindromic RNA duplex were systematically replaced with nucleobase-methylated nucleosides such as 1-methylguanosine (m^1G), N^2-methylguanosine (m^2G), N^2,N^2-dimethylguanosine ($m^2{}_2G$), 1-methylinosine (m^1I), 3-methyluridine (m^3U), N^4-methylcytidine (m^4C), N^6-methyladenosine (m^6A), and N^2,N^2-dimethyladenosine ($m^6{}_2A$). Investigation of the corresponding duplex–hairpin equilibria revealed the methylated nucleotides that provide the potential for secondary structure rearrangements.[60, 61]

Outlook

RNA has great conformational flexibility not only at the tertiary but also at the secondary structure level. Biologists and biochemists have identified RNAs that exploit secondary structure rearrangements for functional control in several organisms. To understand the molecular mechanisms behind these RNA refolding processes, great efforts will be necessary to create powerful approaches that allow real-time structural analysis. NMR spectroscopic methods applied to RNAs with sequence-specific ^{15}N-labeled nucleotides would meet such requirements as information about formation or breakage of single-labeled base pairs should be easy to acquire during the transition from one conformation to another by use of such labels. Structural probing by comparative imino proton NMR spectroscopy as discussed above could assist in selecting the potential candidates for the nucleotide labels within an RNA. Single-nucleotide labeling of RNA is still a major challenge and highly demanding from a chemical point of view. However, recent improvements in the chemical synthesis of oligoribonucleotides are promising and may make site-specifically labeled RNAs readily available soon.[62–66]

Acknowledgements

Financial support from the Austrian Science Fund (Grant no. P15042) is gratefully acknowledged.

Keywords: NMR spectroscopy · nucleotides · RNA · RNA switches · structure elucidation

[1] P. Brion, E. Westhof, *Annu. Rev. Biophys. Biomol. Struct.* **1997**, *26*, 113–137.
[2] X. Zhuang, L. E. Bartley, H. P. Babcock, R. Russell, T. Ha, D. Herschlag, S. Chu, *Science* **2000**, *288*, 2048–2051.
[3] B. Scalvi, M. Sullivan, M. R. Chance, M. Brenowitz, S. A. Woodson, *Science* **1998**, *279*, 1940–1943.
[4] A. A. Szewczak, E. R. Podell, P. C. Bevilacqua, T. R. Cech, *Biochemistry* **1998**, *37*, 11162–11170.

[5] S. A. Woodson, *Cell Mol. Life Sci*. **2000**, *57*, 796 – 808.
[6] J. Pan, D. Thirumalai, S. A. Woodson, *J. Mol. Biol*. **1997**, *273*, 7 – 13.
[7] D. Repsilber, S. Wiese, M. Rachen, A. W. Schröder, D. Riesner, G. Steger, *RNA* **1999**, *5*, 574 – 584.
[8] T. R. Kadesch, M. J. Chamberlin, *J. Biol. Chem.* **1982**, *257*, 5286 – 5295.
[9] M. Golomb, M. J. Chamberlin, *J. Biol. Chem*. **1974**, *249*, 2855 – 2863.
[10] P. F. Agris, *Prog. Nucleic Acid Res. Mol. Biol*. **1995**, *53*, 79 – 129.
[11] M. Wu, I. Tinoco, Jr., *Proc. Natl. Acad. Sci. USA* **1998**, *95*, 11 555 – 11 560.
[12] J. H. A. Nagel, C. W. A. Pleij, *Biochimie* **2002**, *84*, 913 – 922.
[13] W. Zhang, S. J. Chen, *Proc. Natl. Acad. Sci. USA* **2002**, *99*, 1931 – 1936.
[14] R. Russell, D. Herschlag, *J. Mol. Biol*. **2001**, *308*, 839 – 851.
[15] S. K. Silverman, M. L. Deras, S. A. Woodson, S. A. Scaringe, T. R. Cech, *Biochemistry* **2000**, *39*, 12 465 – 12 475.
[16] C. Waldsich, B. Masquida, E. Westhof, R. Schroeder, *EMBO J.* **2002**, *21*, 5281 – 5291.
[17] D. M. Chadalavada, S. E. Senchak, P. C. Bevilacqua, *J. Mol. Biol*. **2002**, *317*, 559 – 575.
[18] Y. Tanaka, T. Hori, M. Tagaya, T. Sakamoto, Y. Kurihara, M. Katahira, S. Uesugi, *Nucleic Acids Res*. **2002**, *30*, 766 – 744.
[19] A. R. Ferre-D'Amare, K. Zhou, J. A. Doudna, *Nature* **1998**, *395*, 567 – 574.
[20] D. van Meerten, G. Girard, J. van Duin, *RNA* **2001**, *7*, 483 – 494.
[21] R. A. Poot, N. V. Tesareva, I. V. Boni, J. van Duin, *Proc. Natl. Acad. Sci. USA* **1997**, *94*, 10 110 – 10 115.
[22] F. J. Grundy, S. M. Rollins, T. M. Henkin, *J. Bacteriol*. **1994**, *176*, 4518 – 4526.
[23] F. J. Grundy, T. M. Henkin, *Front. Biosci.* **2003**, *8*, D20 – D31.
[24] A. M. G. Dirac, H. Huthoff, J. Kjems, B. Berkhout, *Nucleic Acids Res*. **2002**, *30*, 2647 – 2655.
[25] H. Huthoff, B. Berkhout, *Biochemistry* **2002**, *41*, 10 439 – 10 445.
[26] J. H. A. Nagel, A. P. Gultyaev, K. Gerdes, C. W. A. Pleij, *RNA* **1999**, *5*, 1408 – 1419.
[27] A. P. Gultyaev, T. Franch, K. Gerdes, *J. Mol. Biol*. **1997**, *273*, 26 – 37.
[28] K. Gerdes, A. P. Gultyaev, T. Franch, K. Pedersen, N. D. Mikkelsen, *Annu. Rev. Genet*. **1997**, *31*, 1 – 31.
[29] K. Gerdes, P. B. Rasmussen, S. Molin, *Proc. Nat. Acad. Sci. USA* **1986**, *83*, 3116 – 3120.
[30] K. Gerdes, A. Nielsen, P. Thorsted, E. G. H. Wagner, *J. Mol. Biol.* **1992**, *226*, 637 – 649.
[31] K. Gerdes, T. Thisted, J. Martinussen, *Mol. Microbiol.* **1990**, *4*, 1807 – 1818.
[32] F. Franch, K. Gerdes, *Mol. Microbiol.* **1997**, *21*, 1049 – 1060.
[33] F. Franch, A. P. Gultyaev, K. Gerdes, *J. Mol. Biol.* **1997**, *273*, 38 – 51.
[34] J. H. A. Nagel, A. P. Gultyaev, K. J. Öistämö, K. Gerdes, C. W. A. Pleij, *Nucl. Acids Res.* **2002**, *30*, e63.
[35] E. A. Schultes, D. P. Bartel, *Science* **2000**, *289*, 448 – 452.
[36] R. Micura, C. Höbartner in *Bioorganic Chemistry Highlights: From Chemistry to Biology* (Eds.: C. Schmuck, H. Wennemers), Wiley-VCH, Weinheim, **2003**, in press.
[37] C. Höbartner, M.-O. Ebert, B. Jaun, R. Micura, *Angew. Chem.* **2002**, *114*, 619 – 623; *Angew. Chem. Int. Ed.* **2002**, *41*, 605 – 609.
[38] C. Höbartner, R. Micura, *J. Mol. Biol.* **2003**, *325*, 421 – 431.
[39] H. Moine, B. Ehresmann, C. Ehresmann, P. Romby in *RNA Structure and Function* (Eds.: R. W. Simons, M. Grunberg-Manago), Cold Spring Harbor Laboratory Press, NY, **1998**, pp. 77 – 115.
[40] J. Hearst in *Nucleic Acids Structures, Properties, and Function* (V. A. Bloomfield, D. A. Crothers, I. Tinoco Jr.), University Science Books, Sausalito, CA, **2000**, pp. 45 – 78.
[41] J. Xu, J. Lapham, D. M. Crothers, *Proc. Natl. Acad. Sci. USA* **1996**, *93*, 44 – 48.
[42] N. B. Leontis, P. B. Moore, *Biochemistry* **1986**, *25*, 3916 – 3925.
[43] H. A. Heus, O. C. Uhlenbeck, A. Pardi, *Nucleic Acids Res*. **1990**, *18*, 1103 – 1108.
[44] O. Odai, H. Kodama, H. Hiroaki, T. Sakata, T. Tanaka, S. Uesugi, *Nucleic Acids Res*. **1990**, *18*, 5955 – 5960.
[45] W. Pils, R. Micura, *Nucleic Acids Res*. **2000**, *28*, 1859 – 1863.
[46] M.-O. Ebert, B. Jaun, W. Pils, R. Micura, *Helv. Chim. Acta.* **2000**, *83*, 2238 – 2243.
[47] C. Flamm, I. L. Hofacker, S. Maurer-Stroh, P. F. Stadler, M. Zehl, *RNA* **2001**, *7*, 254 – 265.
[48] E. Tostesen, S.-J. Chen, K. A. Dill, *J. Phys. Chem. B*. **2001**, *105*, 1618 – 1630.
[49] M. Zuker, *Curr. Opin. Struct. Biol*. **2000**, *10*, 303 – 310.
[50] S. R. Morgan, P. G. Higgs, *J. Chem. Phys*. **1996**, *105*, 7152 – 7157.
[51] D. H. Mathews, J. Sabina, M. Zuker, D. H. Turner, *J. Mol. Biol*. **1999**, *288*, 911 – 940.
[52] S.-J. Chen, K. A. Dill, *Proc. Natl. Acad. Sci. USA* **2000**, *97*, 646 – 651.
[53] N. Breton, C. Jacob, P. Daegelen, *J. Biomol. Struct. Dyn*. **1997**, *14*, 727 – 740.
[54] C. Gaspin, E. Westhof, *J. Mol. Biol*. **1995**, *254*, 163 – 174.
[55] http://www.tbi.univie.ac.at/∼ivo/RNA/, **1994** – **2001**, free software, version 1.4.
[56] S. Wuchty, W. Fontana, I. L. Hofacker, P. Schuster, *Biopolymers* **1999**, *49*, 145 – 165.
[57] C. Flamm, W. Fontana, I. L. Hofacker, P. Schuster, *RNA* **2000**, *6*, 325 – 338.
[58] M. Helm, H. Brulé, F. Degoul, C. Cepanec, J.-P. Leroux, R. Giegé, C. Florentz, *Nucleic Acids Res.* **1998**, *26*, 1636 – 1643.
[59] M. Helm, R. Giegé, C. Florentz, *Biochemistry* **1999**, *38*, 13 338 – 13 346.
[60] R. Micura, W. Pils, C. Höbartner, K. Grubmayr, M.-O. Ebert, B. Jaun, *Nucleic Acids Res*. **2001**, *29*, 3997 – 4005.
[61] C. Höbartner, C. Kreutz, E. Flecker, E. Ottenschläger, W. Pils, K. Grubmayr, R. Micura, *Monatsh. Chem.* **2003**, *134*, 851 – 873.
[62] R. Micura, *Angew. Chem.* **2002**, *114*, 2369 – 2373; *Angew. Chem. Int. Ed.* **2002**, *41*, 2265 – 2269.
[63] S. Pitsch, P. A. Weiss, L. Jenny, A. Stutz, X. Wu, *Helv. Chim. Acta* **2001**, *84*, 3773 – 3795.
[64] S. A. Scaringe, *Methods* **2001**, 23, 206 – 217.
[65] J. Milecki, A. Földesi, A. Fischer, R. W. Adamiak, J. Chattopadhyaya, *J. Labelled Compd. Radiopharm.* **2001**, *44*, 763 – 783.
[66] X. Ariza, J. Vilarrasa, *J. Org. Chem.* **2000**, *65*, 2827 – 2829.

Received: May 20, 2003 [M664]

